Journal of GeoEngineering, Vol. 14, No. 3, pp. 121-128, September 2019
http://dx.doi.org/10.6310/jog.201909_14(3).1

STRUCTURAL MODELLING IN FINITE ELEMENT ANALYSIS OF DEEP EXCAVATION

Suched Likitlersuang [1], Chhunla Chheng [2], and Suraparb Keawsawasvong [3*]

ABSTRACT

Due to advancements in computation, most deep excavation projects are now designed based on the results of numerical analysis. However, designers are usually careless about structural modelling. This study presents the effect of structural modelling on wall deformations of deep excavation. A 3D finite element method was employed to model the problem, and a residential building project located in Bangkok was selected for the study. Structural models, including diaphragm wall, diagonal braces, and bored piles, were the focus of study, which indicates that the types of elements used to model the structure system significantly affect the finite element analysis result.

Key words: Finite element modelling, deep excavation, diaphragm wall, diagonal bracing, bored pile.

1. INTRODUCTION

Wall deformation during excavation is caused by the active pressure of surrounding soils acting on walls during the removal of soils inside the excavation pit. Clough and O'Rourke (1990) explained the behaviour of the wall deformation in response to excavation stages as presented in Fig. 1. Two types of deformation, cantilever and deep inward, were identified. The cantilever type appears at the early stage of excavation, when no struts or slabs have yet been installed. On the other hand, a deep inward pattern is exhibited after the bracing systems have been installed and the excavation has advanced to deeper depth. Each type of deformation leads to a different type of ground settlement profile as depicted in Fig. 1. Similar findings were also obtained by Ou *et al.* (1993). They noted that the maximum lateral wall movement (δ_{hm}) often occurred near the excavation surface and fell within the range of 0.002 ~ 0.005 of excavation depth.

In deep excavation, many structures are employed to support the surrounding soils. Specifically, struts, wailings, and exiting piles are required in underground construction. Hsiung *et al.* (2016) modelled deep excavation in Taiwan with 3D finite element modelling. In their studies, D-walls (diaphragm wall) were modelled with plate elements. The study emphasised the corner effect, and the results corresponded well with the measured lateral wall deformation. Hsieh *et al.* (2016) studied the effect of buttress walls in reducing deformation of the diaphragm walls in two case studies in Taipei. Several parametric studies were conducted to understand the behaviour of buttress walls in reducing deformation of

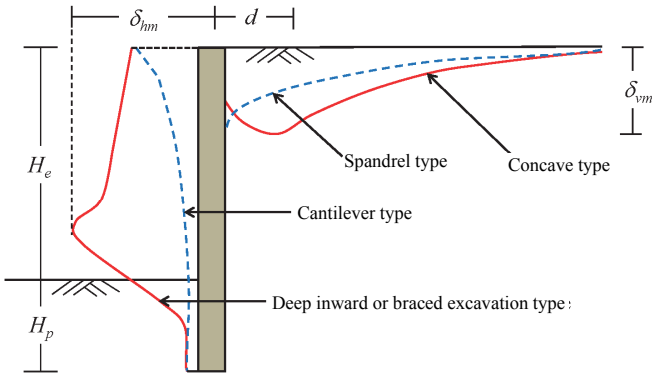

H_e = hieght of the wall, H_p = depth of the embeeded part of the wall, δ_{hm} = maximum horizontal displacmenet, δ_{vm} = maximum vertical displacmenet and d = distance from the wall to the maximum vertical displacmenet

Fig. 1 Types of wall movement and ground surface settlement (Ou *et al.* 1993)

the D-wall. These studies consistently modelled the D-wall with plate elements. The simulations projected wall deformation close to the monitored results. Other studies, including Hsieh *et al.* (2012) and Hsieh and Ou (2016), employed linear elastic of beam to model the diaphragm walls in their 3D analyses. However, the models of diagonal bracing and piles were ignored in those aforementioned studies. In addition, Jamsawang *et al.* (2017) observed and simulated lateral movements and strut forces of deep cement mixing (DCM) walls, which were modelled using non-porous elastic volume elements. Struts were modelled by beam elements while slabs were modelled with plate elements, and the predicted lateral wall movements agreed well with the measured values. Furthermore, Hou *et al.* (2009) modelled the North Square underground shopping centre of Shanghai South Railway Station using 3D FEM in Abaqus software. In the problem, soils were modelled using 3D linear-order solid element with anisotropic elastic stiffness, whereas D-wall was modelled by shell element as an elastic material. In addition, the FE model incorporates the existing bored

Manuscript received October 6, 2018; revised February 15, 2019; accepted March 23, 2019.
[1] Professor, Centre of Excellence in Geotechnical and Geoenvironmental Engineering, Department of Civil Engineering, Faculty of Engineering, Chulalongkorn University, Bangkok, Thailand.
[2] Former Master's student, Department of Civil Engineering, Faculty of Engineering, Chulalongkorn University, Bangkok, Thailand.
[3*] Lecturer (corresponding author), Thammasat School of Engineering, Thammasat University, Pathumthani, Thailand (e-mail: suraparb@hotmail.com).

piles and girders, which were modelled by beam elements at the same time. Subsequently, Dong *et al.* (2013, 2014) modelled the same site in Shanghai with 3D FE model taking into account of small strain stiffness of soil. The soil and D-wall were modelled by solid element using 8-node hexahedral elements with reduced integration (C3D8R) in Abaqus software. In their studies, the bored piles were modelled by the beam element, but the girders were ignored in the model. In general, both predictions of Hou *et al.* (2009) and Dong *et al.* (2013, 2014) agreed well with the field measurements.

From the aforementioned studies, although it is not necessary to model all the structures in the analysis, some structures may have a greater effect on the analysis while some may have a lesser effect on the analysis results. Therefore, this study aims to provide the information on the use of finite element analysis for structural modelling of deep excavation. The structural models include types of elements for modelling D-walls as well as choices for modelling diagonal bracing and bored piles. Underground construction of a residential building located in downtown Bangkok was selected as a case study for verification of the model. A PLAXIS 3D version AE.02 was used for modelling and analysis. Finally, a suggestion on the choices of finite element analysis for structure modelling of deep excavation is provided.

2. BANGKOK SUBSOIL AND CONSTITUTIVE MODELLING

Bangkok is located on the low flat of the Chao Praya Delta in the central plain region of Thailand. The soil is generally divided into 7 different layers, including Made Ground (MG), Bangkok Soft Clay (BSC), Medium Clay (MC), First Stiff Clay (1st SC), Clayey Sand (CS), Second Stiff Clay (2nd SC) and Hard Clay (HC) (Likitlersuang *et al.* 2013a) as shown in Table 1. Extensive studies of Bangkok clay behaviours have been carried out by the Asian Institute of Technology and Chulalongkorn University (Likitlersuang *et al.* 2013a, 2013b, 2013c, 2018; Surarak *et al.* 2012). In terms of groundwater condition, Bangkok suffered from a drawdown of pore water pressure observed by Likitlersuang *et al.* (2013b) during the construction of the Bangkok MRT Blue Line, due to the deep well pumping many years ago, and illustrated in Fig. 2. The pore water distribution was modelled as a drawdown condition in this study.

The Hardening Soil Model (HSM) is one of the advanced constitutive soil models implemented in commercial finite element software. The model adopts the Duncan-Chang hyperbolic stress strain (Duncan and Chang 1970) where stiffness is stress-dependent. Further details of the model can be found in Schanz *et al.* (1999).

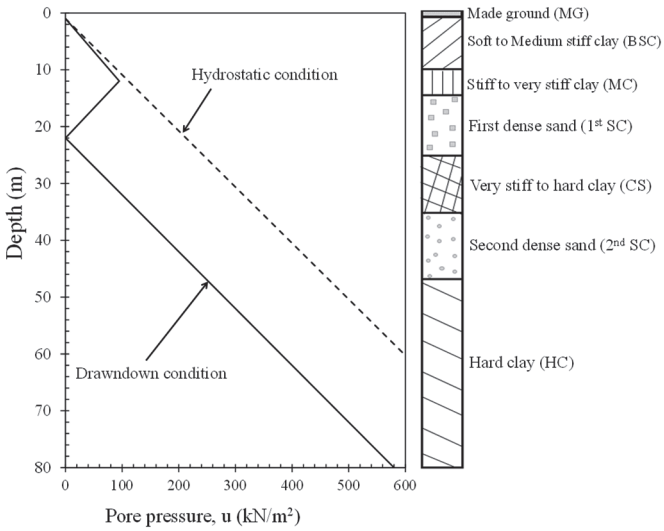

Fig. 2 Pore pressure in Bangkok subsoils (Likitlersuang *et al.* 2013a)

Surarak *et al.* (2012) studied the HSM soil models for Bangkok clays. Based on the results from oedometer and triaxial tests, the HSM soil parameters were numerically calibrated. Likitlersuang *et al.* (2013b, 2018) provided a complete set of HSM parameters for Bangkok subsoils, with explanations, as tabulated in Table 1 and Table 2 respectively. In this study, the HSM model adopted from Likitlersuang *et al*. (2013a) were used to characterise the soft and stiff Bangkok clays. A list of the input parameters for Bangkok subsoils is presented in Table 1.

3. FINITE ELEMENT ANALYSIS OF DEEP EXCAVATION

The use of numerical methods has recently become more powerful tool in geotechnical engineering, however, only two-dimensional (2D) finite element analysis (FEA) has been extensively employed in practice. Simplified assumptions, such as plane strain or axi-symmetry, are made in 2D FEA but, only a few cases of deep excavation can be reasonably simplified for modelling in 2D FEA. For example, the 3D effect can be neglected only for rectangular excavations whose length-to-width ratio (*L/W*) is larger than 6 (Faheem *et al.* 2004). However, by observation from an excavation with *L/W* is greater than 6 but measurement data near the corner, the lateral wall displacement is still highly affected by the corner (Hsiung *et al.* 2018). In general, the effect of 3D shall be relied on the distance from the corner of excavation. Furthermore, features which cannot be modelled in 2D FEA include corner effect,

Table 1 Input parameters for HSM (after Likitlersuang *et al.* 2013b)

Soil type	Depth (m)	γ_b (kN/m^3)	c' (kN/m^2)	ϕ' (°)	ψ' (°)	E_{50}^{ref} (MPa)	E_{oed}^{ref} (MPa)	E_{ur}^{ref} (MPa)	ν_{ur}	m	K_0^{nc}	R_f	R_{inter}
MG	0.00 ~ 1.29	18.0	1	25	0	45.60	45.60	136.8	0.2	1	0.58	0.9	0.7
BSC	1.29 ~ 10.0	16.5	1	23	0	0.80	0.85	8.0	0.2	1	0.70	0.9	0.7
MC	10.0 ~ 14.5	17.5	10	25	0	1.65	1.65	5.4	0.2	1	0.60	0.9	0.7
1st SC	14.5 ~ 25.0	19.5	25	26	0	8.50	9.00	30.0	0.2	1	0.50	0.9	0.7
CS	25.0 ~ 35.4	19.0	1	27	0	38.00	38.00	115.0	0.2	0.5	0.55	0.9	0.7
2nd SC	35.4 ~ 47.2	20.0	25	26	0	8.50	9.00	30.0	0.2	1	0.50	0.9	0.9
HC	47.2 ~ 80.0	20.0	40	24	0	30.00	30.00	120.0	0.2	1	0.50	0.9	0.9

Table 2 HSM parameters explanation

Parameter symbol	Parameter description	Parameters evaluation
ϕ'	Internal friction angle	Slope of failure line from Mohr-Coulomb model
c'	Cohesion	y-intercept of failure line from Mohr-Coulomb model
ψ'	Dilatancy angle	Ratio of $d\varepsilon_v^p$ and $d\varepsilon_s^p$
E_{50}^{ref}	Reference secant stiffness from drained triaxial test	y-intercept in $\log(\sigma_3/p^{ref}) - \log(E_{50})$ curve
E_{oed}^{ref}	Reference tangent stiffness for oedometer primary loading	y-intercept in $\log(\sigma_1/p^{ref}) - \log(E_{oed})$ curve
E_{ur}^{ref}	Reference unloading/reloading stiffness	y-intercept in $\log(\sigma_3/p^{ref}) - \log(E_{ur})$ curve
ν_{ur}	Unloading/reloading Poisson's ratio	0.2 (default setting)
m	Exponential power	Slope of trend-line in $\log(\sigma_3/p^{ref}) - \log(E_{50})$ curve
K_0^{nc}	Coefficient of earth pressure at rest (NC state)	$1 - \sin\phi'$ (default setting)
R_f	Failure ratio	$(\sigma_1 - \sigma_3)_f / (\sigma_1 - \sigma_3)_{ulf}$

Remarks: σ_1 is major principle stress (kN/m^2); σ_3 is minor principle stress (kN/m^2); p^{ref} is reference pressure (100 kN/m^2)

complex condition, and irregular shape of excavation. Chheng and Likitlersuang (2018) provided evidence that 3D FE modelling is effective for deep excavation analysis in Bangkok. In the previous study, two deep excavation projects in Bangkok were used to validate the performance of 3D FE modelling. However, there is a question about the effect of the structural models on the results of FEA; therefore, this study extends the previous study (Chheng and Likitlersuang 2018), focusing on the structural modelling of 3D FEA in a deep excavation.

3.1 General Information about Deep Excavation Project

Silom is a very busy area of Bangkok city, consisting of many commercial and residential buildings. Underground construction work for high-rise residential building project in Silom was selected in this study. The top view of the project layout is illustrated in Fig. 3(a). The construction site is rectangular in shape with 57.4 m long and 23.5 m wide (L/W = 2.44). The 2D FEA may not be capable of effectively handling the interconnection of the whole construction area especially near the movement of wall near the corner of excavation. The building consists of 3 levels of underground floors as shown in Fig. 3(b). The surrounding soil is supported by 0.8 m thick diaphragm walls (D-walls), with a depth of 19 m from top to bottom. Some D-wall panels are supported by barrette piles of the same thickness to a depth of 55 m below ground level. Noted that the function of barrette pile is to carry the load of diaphragm wall. Since the barrette pile can be constructed using the same equipment as diaphragm wall (*i.e.,* grab and cutter). It is convenient and less time-consuming for the contractor to use the diaphragm wall and barrette pile system as retaining wall. Two levels of strut bracing system are used to laterally support the walls. Bored piles had already been installed before the excavation started. The maximum depth of excavation was 11.55 m below the ground surface, and a bottom-up construction method was adopted.

The site was modelled and analysed using 3D FEA. A 10-noded tetrahedron element with quadratic displacement function was selected to discretise the soil volumes (Brinkgreve *et al.* 2015). The 3D model with a dimension of 140 × 103 × 80 m has a total of 264,163 elements and an average size of 2.005 m as displayed in Fig. 4. The side boundaries were set as lateral displacement constraints, whereas the bottom boundaries were fixed supports. Noted that the effect of boundary conditions was studied by observing the deformation near boundaries and no boundary effect was observed.

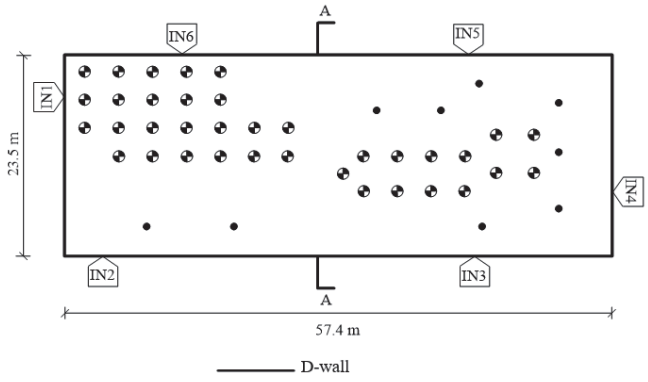

(a) Top view

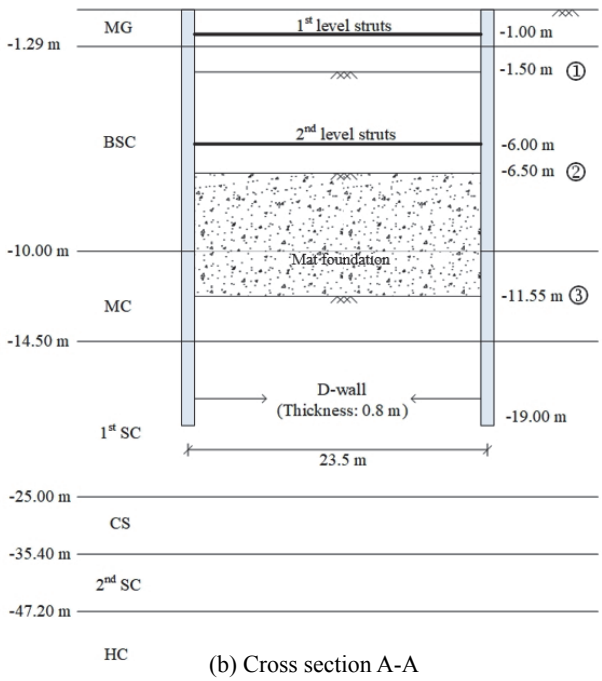

(b) Cross section A-A

Fig. 3 Silom residential project

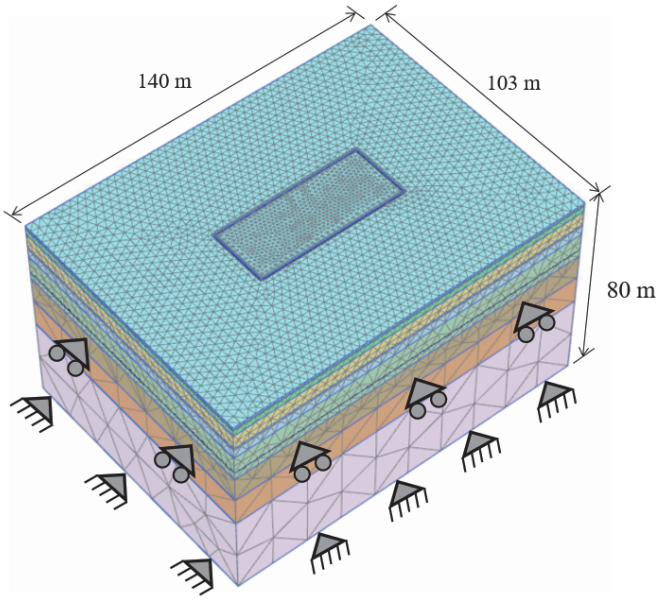

Fig. 4 Geometry and finite element mesh of excavation problem (264,163 elements with the average size of 2.005 m)

The soil layers beneath the construction side consist of 7 layers, and are typical of subsoil layers in Bangkok. The Hardening Soil Model (HSM) and its parameters, as shown in Table 1, following Likitlersuang *et al.* (2013b), were adopted in this study.

3.2 Construction Sequences

The underground construction of this project started with installation of D-walls surrounding the excavation area and bored piles. Firstly, the soil was excavated to a level of 1.50 m below ground level. Before proceeding to the next level of excavation, bracings were installed at a level of 1.0 m deep (1st level). Then the excavation continued to 6.5 m below ground level. Again, bracings were installed; this time, 6.0 m below level 0.00 (2nd level). Next, the excavation proceeded to the final depth of 11.55 m below ground surface. Then 200 mm of lean concrete was cast at the bottom of the excavation floor and overlaid by 5,050 mm thick of concrete mat foundation. The finished depth was 8.65 m. The excavation was finished, and the bottom-up construction was started with the removal of the second level bracing system, and B2 slab was cast at a depth of 5.85 m. Then, the B1 slab was cast and the 1st level of bracing systems were removed to complete the underground construction works. All construction sequences are summarised in Table 3 and Fig. 3(b). Since there are no excavation activities in the construction sequences 4 ~ 6 (the maximum desired depth is reached in stage 3). In this study, the simulations were performed for the construction sequences 1 ~ 3 as denoted in Table 3. Noted that small movements might occur during casting the D-wall; however, the effect of the D-wall installation was not considered in the finite element modelling.

3.3 Structural Modelling Choices

In an underground construction project process, many structural elements are employed to support the surrounding soils. To optimise the modelling and calculation efforts, engineers should minimise or simplify structural models which provide less influence on the analysis results, especially on load and deformation characteristics of the D-wall.

In this study, the D-wall modelling options were considered first. The D-wall is a finite-thickness concrete structure commonly designed using elastic material. Everaars and Peters (2013) indicated that a D-wall could be modelled with an elastic beam element in 2D or a linear elastic non-porous volume element. Therefore, a simplified elastic structural element (plate element) and a solid volume element were selected to model the D-wall in this study, as shown in Figs. 5(a) and 5(b), respectively. The thickness of the D-wall is not yet modelled three-dimensionally by plate elements. On the contrary, the thickness of the D-wall is usually geometrically modelled for volume elements; therefore, it is not practical to vary the thickness of the D-wall in this option, unlike in the plate element option. In addition, modelling the D-wall using volume elements takes more effort. The rigidity of concrete is mainly controlled by modulus of elasticity (E), Poisson's ratio (ν), thickness (t), and unit weight of plate (γ) (the difference between the unit weight of concrete and unit weight of soil) to account for

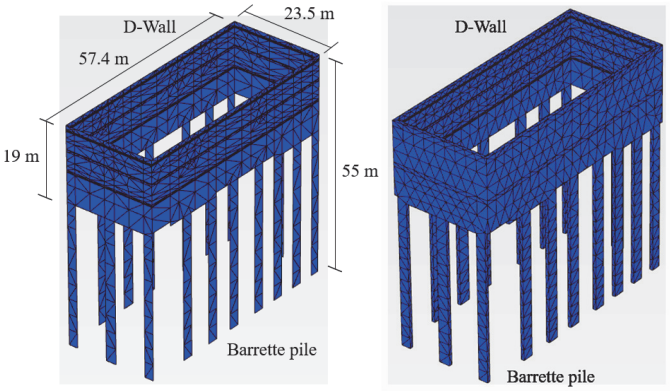

(a) Plate element (b) Volume elements

Fig. 5 Models of D-wall

Table 3 Underground construction sequences of Silom residential project

Sequences	Construction activities
1	Wish-in-place of D-wall, bored piles, and excavation to the depth of 1.5 m
2	Install and preload the 1st level of bracing system at depth of 1.00 m and excavated to the depth of 6.5 m
3	Install and preload the 2nd level of bracing system at depth of 6.00 m and excavate to the depth of 11.55 m
4	Finish lean concrete and mat foundation at depth of 6.50 ~ 11.55 m
5	Remove 2nd level of bracing system and cast B2 slab at depth of 5.85 m
6	Cast B1 slab at depth of 3.05 m and remove the 1st level of bracing system

Remarks: Preloads at both level of struts are 30% of design load; 2) The numerical simulations are only performed for the excavation processes (sequences 1 to 3)

the non-volume elements (Hsiung *et al.* 2016a). Input parameters for plate elements are summarised in Table 4. Nevertheless, for the volume element modelling option in this study, the D-wall was modelled by tetrahedral volume elements. The volumes adopted linear elastic and non-porous parameters for drainage type as tabulated in Table 5.

Table 4 Simplified elastic structural element (plate element) parameters for diaphragm wall system (Chheng and Likitlersuang 2018)

Parameters	d (m)	γ (kN/m^3)	E (kN/m^2)	ν_{12}
D-wall and barrette pile	0.8	16	24,800	0.15
Slabs	1.0	23	24,800	0.15

Table 5 Volume element parameters for diaphragm wall system (Chheng and Likitlersuang 2018)

Parameters	d (m)	γ (kN/m^3)	E (kN/m^2)	ν_{12}	Drainage type
D-wall and barrette pile (Linear elastic)	0.8	23	24,800	0.15	Non-porous

The second consideration in this study focused on diagonal bracing at the end of each strut. Diagonal braces are used to reduce the spans between the struts, and are usually installed at a 45° angle to the struts. Two options were studied: modelling with and without diagonal bracing, as illustrated in Figs. 6(a) and 6(b), respectively. In PLAXIS 3D modelling, the diagonal bracing option can be activated or deactivated for different cases – those with and without diagonal bracing, respectively. Struts and wailings were modelled by beam elements, and their input parameters are tabulated in Table 6. Noted that to model the diagonal bracing system more realistic, the beam element was selected instead of a simplified anchor element in this study.

Lastly, the model for existing bored piles was considered. Bored piles are structures which are used to support superstructure loads. Piles are usually installed before the excavation and they can reduce both horizontal movements and settlement behind the retaining wall (McNamara 2011). In this study, two optional models with and without modelling of bore piles were looked at in this study as presented in Figs. 7(a) and 7(b), respectively. Bored piles were modelled by embedded beam elements, which require the input parameters found in Table 7. The embedded beam consists of beam elements with special interface elements providing the

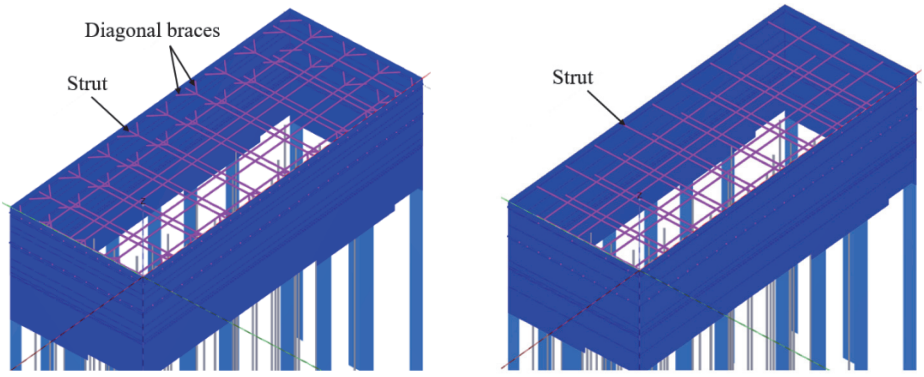

(a) Model with diagonal braces (b) Model without diagonal braces

Fig. 6 Models of construction work

Table 6 Beam element parameters for bracing system (Chheng and Likitlersuang 2018)

Parameters	A (m^2)	γ (kN/m^3)	E (kN/m^2)	I_3 (m^4)	I_2 (m^4)
Steel strut (400 × 400 × 172 kg/m)	2.19×10^{-2}	77.15	210 000	2.24×10^{-4}	6.66×10^{-4}
Steel wailings (400 × 400 × 172 kg/m)	2.19×10^{-2}	77.15	210 000	6.66×10^{-4}	2.24×10^{-4}

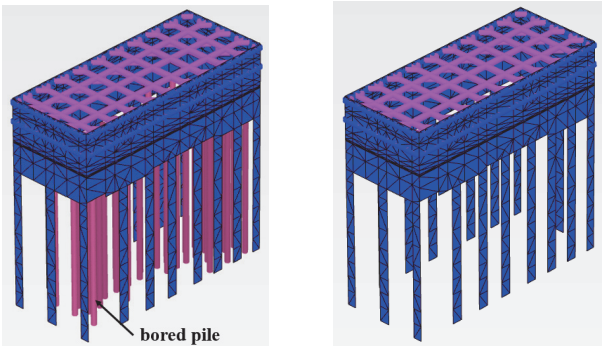

(a) Model with bored piles (b) Model without bored piles

Fig. 7 Models of construction work

Table 7 Embedded beam parameters for bored piles

E (kN/m^2)	γ (kN/m^3)	Type	Diameter (m)	Skin resistance (kN/m)	End resistance (kN)
24,800	23	Massive circular pile	1.2	260	2,443
24,800	23	Massive circular pile	0.8	173	1,086

Remarks: The average skin friction (f_s) = 69 kN/m^2 and the end bearing (q_b) = 2,160 kN/m^2

interaction between pile and the surrounding soil. The interaction may involve a skin resistance (f_s) and an end resistance (q_{end}). Noted that the skin friction and end resistance were approximated from $f_s = \alpha s_{u,ave} \pi D$ and $q_{end} = 9 s_{u,end} \pi D^2/4$, where $s_{u,ave}$ and $s_{u,end}$ are the average undrained shear strength of soil through the plie length and the undrained shear strength of soil at pile tip location, respectively.

4. ANALYSIS RESULTS

4.1 D-wall Modelling

This section aims to show the results of wall deformation from the different methods used for modelling the D-walls. The simulations were performed following the construction sequence as described in Table 3 and Fig. 3(b). For the plate elements and volume elements modelling of D-walls, the wall movements are plotted and compared with monitoring data as shown in Fig. 8, in which the symbol numbers in circle are referred to the construction stages as described in Table 3 and Fig. 3(b). The stages 2 and 3 data, measured by inclinometers (IN1 and IN2) are included in Fig. 8, while the locations of the inclinometers are referred to in Fig. 3(a). The results reveal that the estimated D-wall deformation modelled by plate elements tends to be a little larger than that modelled by volume elements in all stages of construction. Additionally, the modelling D-wall by plate elements is more convenient for the designer. Since bending moment and shear force can be obtained directly from the plate elements, whereas the volume elements present the internal stresses. To calculate the bending moment and shear force from the internal stresses requires more efforts on post-processing calculation. A separated numerical code may be required for the calculation. Therefore, the selection of which type of model to use for predicting D-wall deformation is a decision for the engineers on a case-by-case basis.

4.2 Diagonal Bracing Modelling

Figure 9 presents the numerical results of the wall deformation for each construction stage for both optional models of diagonal bracing (*i.e.,* with and without modelling the diagonal braces), in which the symbol numbers in circle are referred to the construction stages as described in Table 3 and Fig. 3(b). The simulations are also compared with the data measured from inclinometers at IN1 and IN2. The results indicate that the differences are very insignificant. In this study, it was found that the diagonal braces can be ignored in order to reduce the effort required and the calculation time. However, in a complicated excavation site, such as one with an irregular shape and heavier diagonal bracing modelling may be required.

4.3 Bored Pile Modelling

The bored pile modelling results are extracted and plotted in Fig. 10 for both options (*i.e.,* with and without piles modelling), in which the symbol numbers in circle are referred to the construction stages as described in Table 3 and Fig. 3(b). The simulations are also compared with the data measured from inclinometers at IN1 and IN2 as shown in Figs. 10(a) and 10(b), respectively. Noted that the IN1 is closed to the group of bored piles, whereas the IN2 is located far from the bored piles. In general, the model including bored piles was found to reduce the horizontal movements of wall, which also agree with McNamara (2001). In fact, the wall deformation was influenced by the presence of the bored piles only near the tip of the D-wall (Fig. 10(a)). In the models, most of the pile heads were at levels lower than the excavation depth. However, the presence of piles under the excavation site could affect the heaving stability as pointed out by McNamara (2001). This may need further study in the future.

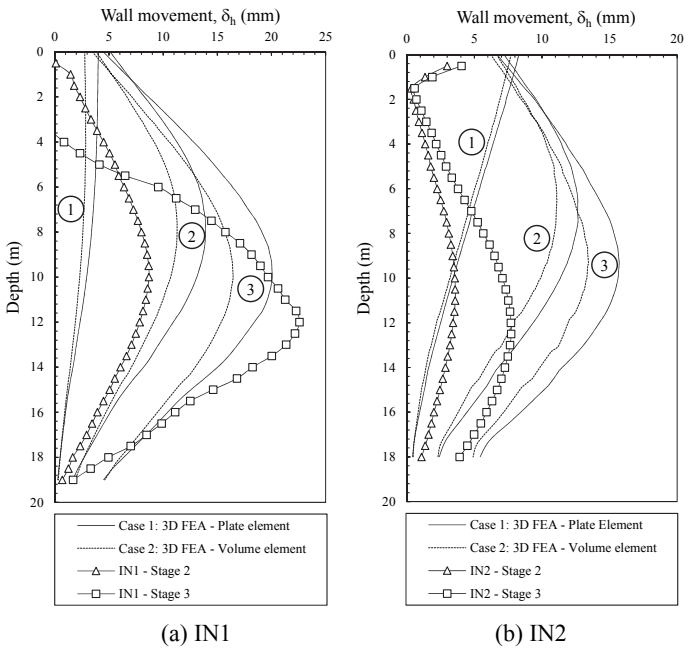

(a) IN1 (b) IN2

Fig. 8 Effect of D-wall modelling on lateral wall movement

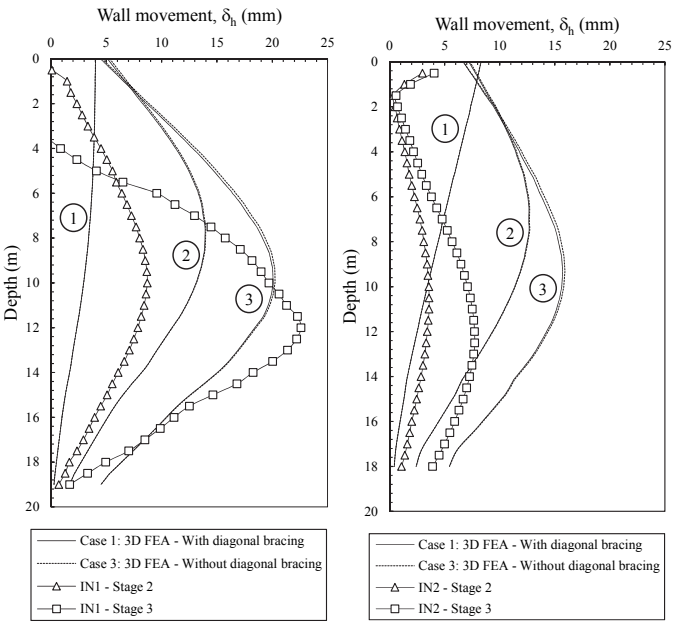

(a) IN1 (b) IN2

Fig. 9 Comparison between models with and without diagonal bracing

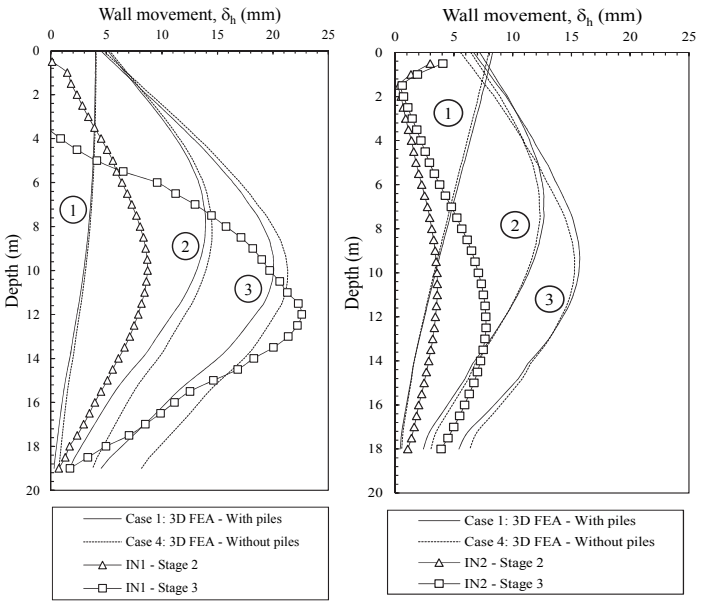

(a) IN1 (b) IN2

Fig. 10 Comparison between models with and without bored piles

5. DISCUSSIONS AND CONCLUSIONS

3D Finite Element Analysis (3D FEA) has become an important numerical tool in the geotechnical engineering field due to the power of today's computer resources. A great deal of calculation effort is required in 3D analysis; hence, an optimised model is needed in order to reduce the calculation time. Table 8 summaries the calculation times influenced by the structural modelling options. In this study, which looked at the underground construction of a residential building, a project in downtown Bangkok was selected as the focus of a case study to investigate the effects of structural modelling, including D-wall modelling, diagonal struts and existing bored piles. Some highlights from this study can be concluded and discussed as follow:

(1) D-walls can be modelled by plate elements or volume elements. It was found that the wall deflection is larger when the wall is modelled by plate elements. This difference of wall movements between modelling D-wall by plate elements and volume elements agrees well with previous studies such as Zdravkovic *et al.* (2005) and Dong *et al.* (2014). However, the use of volume elements requires more effort for modelling the D-wall than plate elements. Such effort includes the modelling time, complexity, calculation time, and results extraction (Chheng and Likitlersuang 2018). In this study, the calculations took 124 minutes for the volume element model, while the calculations took 70 minutes for the plate element model (approximately calculation time was reduced by half) as presented in Table 8.

(2) In practice, diagonal bracing is commonly used to prevent the damage from bucking, which can occur at the wales, connected to the D-wall. In this exercise, it was found that the diagonal bracing could be ignored to reduce the modelling efforts and time consumption, since the braces did not contribute much to wall deformation. Even though the calculation times for the cases with and without diagonal bracing are not much different (see Table 8), the modelling of diagonal braces may be required for more complex sites, such as one with an irregular shape and heavier diagonal bracing. This should be elaborated in the future.

(3) In general, the small differences of wall movements were observed when including bored piles in the model. However, the bored piles can be significantly influenced in the modelling especially at the deeper excavation zone, where the D-walls are near the pile head. Moreover, when bored piles are activated in the model, the calculation time can be significantly increased compared to cases in which bored piles are deactivated. Based on this study, the simulations took 70 minutes for the model with bored poles, while the simulations took only 54 minutes for the model without bored pile (16 minutes difference) as shown in Table 8. It is recommended that the study of bored piles modelling should be elaborated in the future such as modelling of heaving problem and the effect of pile head location.

(4) It is aware from Figs. 8 to 10 that it has significant differences between field measurements and numerical results for various stages of different sections, no matter which model used for the diaphragm wall, with or without modelling diagonal bracing and simulating the piling works inside the excavation or not. Thus, these factors are recognised not to be main reasons for the difference. Therefore, it is suggested that explorations on impacts from small strain characteristics of soils (Likitlersuang *et al.* 2013c) and axial stiffness of the strut shall be carried out in the future. Moreover, the difference of locations of selected cross section for analyses and monitoring is also a possible reason leading to the difference.

ACKNOWLEDGEMENTS

This research was supported by the Thailand Research Fund Grant No. DBG-6180004 and the Ratchadapisek Sompoch Endowment Fund (2019), Chulalongkorn University (762003-CC). The authors would like to thank Lt. Col. Dr. Chanaton Surarak and Dr. Boonlert Siribumrungwong for providing useful information throughout the research. The second author wishes to thank the AUN/SEED-Net (JICA) for a scholarship during his study.

Table 8 Calculation time influenced by structural modelling

Case	D-wall model	Diagonal bracing	Bored piles	Calculation time (minutes)
1	Plate element	Yes	Yes	70
2	Volume element	Yes	Yes	124
3	Plate element	No	Yes	65
4	Plate element	Yes	No	54

Remarks: 3D FE calculations were conducted using Intel® Core™ i7-6500U CPU@2.50GHz

REFERENCES

Brinkgreve, R.B.J., Kumarswamy, S., Swolfs, W.M., Waterman, D., Chesaru, A., and Bonnier, P.G., *et al.,* (2015) *PLAXIS.* PLAXIS bv, The Netherlands.

Chheng, C. and Likitlersuang, S. (2018). "Underground excavation behaviour in Bangkok using three-dimensional finite element method." *Computers and Geotechnics*, **95**, 68-81. https://doi.org/10.1016/j.compgeo.2017.09.016

Clough, G.W. and O'Rourke, T.D. (1990). "Construction-induced movements of insitu walls." *Proceedings of the Design and Performance of Earth Retaining Structures,* Ithaca, New York, 439-470.

Dong, Y., Burd, H., Houlsby, G., and Hou, Y. (2014). "Advanced finite element analysis of a complex deep excavation case history in Shanghai." *Frontiers of Structural and Civil Engineering*, **8**, 93-100. https://doi.org/10.1007/s11709-014-0232-3

Dong, Y., Burd, H., Houlsby, G., and Xu, Z. (2013). "3D FEM modelling of a deep excavation case considering small-strain stiffness of soil and Thermal shrinkage of concrete." *Proceedings of the International Conference on Case Histories in Geotechnical Engineering*, Chicago, Illinois.

Duncan, J.M. and Chang, C.Y. (1970). "Nonlinear analysis of stress and strain in soils." *Journal of the Soil Mechanics and Foundations Division*, ASCE, **96**, 637-659.

Everaars, M.J.C. and Peters, M.G.J.M. (2013). "Finite element modelling of D-wall supported excavations." *Proceedings of the 18th International Conference on Soil Mechanics and Geotechnical Engineering*, Paris, pp. 711-714.

Faheem, H., Cai, F., and Ugai, K. (2004). "Three-dimensional base stability of rectangular excavations in soft soils using FEM." *Computers and Geotechnics*, **31**, 67-74. https://doi.org/10.1016/j.compgeo.2004.02.005

Hou, Y., Wang, J., and Zhang, L. (2009). "Finite-element modeling of a complex deep excavation in Shanghai." *Acta Geotechnica*, **4**, 7-16. https://doi.org/10.1007/s11440-008-0062-3

Hsieh, P.G. and Ou, C.Y. (2016). "Simplified approach to estimate the maximum wall deflection for deep excavations with cross walls in clay under the undrained condition." *Acta Geotechnica*, **11**(1), 177-189. https://doi.org/10.1007/s11440-014-0360-x

Hsieh, P.G., Ou, C.Y., and Hsieh, W.H. (2016). "Efficiency of excavations with buttress walls in reducing the deflection of the diaphragm wall." *Acta Geotechnica*, **11**(5), 1087-1102. https://doi.org/10.1007/s11440-015-0416-6

Hsieh, P.G., Ou, C.Y., and Lin, Y.L. (2012). "Three-dimensional numerical analysis of deep excavations with cross walls." *Acta Geotechnica*, **8**, 33-48. https://doi.org/10.1007/s11440-012-0181-8

Hsiung, B.C.B., Yang, K.H., Aila, W., and Hung, C. (2016). "Three-dimensional effects of a deep excavation on wall deflections in loose to medium dense sands." *Computers and Geotechnics,* **80**, 138-151. https://doi.org/10.1016/j.compgeo.2016.07.001

Hsiung, B.C.B., Yang, K.H., Wahyuning A., and Ge, L. (2018), "Evaluation of the wall deflections of a deep excavation in Central Jakarta using three-dimensional modeling." *Tunnelling and Underground Space Technology*, **72**, 84-96. https://doi.org/10.1016/j.tust.2017.11.013

Jamsawang, P., Jamnam, S., Jongpradist, P., Tanseng, P., and Horpibulsuk, S. (2017). "Numerical analysis of lateral movements and strut forces in deep cement mixing walls with top-down construction in soft clay." *Computers and Geotechnics*, **88**, 174-181. https://doi.org/10.1016/j.compgeo.2017.03.018

Likitlersuang, S., Pholkainuwatra, P., Chompoorat, T., and Keawsawasvong, S. (2018), "Numerical modelling of railway embankments for high-speed train constructed on soft soil." *Journal of GeoEngineering*, TGS, **13**(3). https://doi.org/10.6310/jog.201809_13(3).6

Likitlersuang, S., Surarak, C., Wanatowski, D., Oh, E., and Balasubramaniam, A. (2013a). "Geotechnical parameters from pressuremeter tests for MRT Blue Line Extension in Bangkok." *Geomechanics and Engineering*, **5**, 99-118. https://doi.org/10.12989/gae.2013.5.2.099

Likitlersuang, S., Surarak, C., Wanatowski, D., Oh, E., and Balasubramaniam, A. (2013b). "Finite element analysis of a deep excavation: a case study from the Bangkok MRT." *Soils and Foundations*, **53**, 756-773. https://doi.org/10.1016/j.sandf.2013.08.013

Likitlersuang, S., Teachavorasinskun, S., Surarak, C., Oh, E., and Balasubramaniam, A. (2013c). "Small strain stiffness and stiffness degradation curve of Bangkok Clays." *Soils and Foundations*, **53**, 498-509. https://doi.org/10.1016/j.sandf.2013.06.003

McNamara A.M. (2001). *Influence of Heave Reducing Piles on Ground Movements around Excavations.* Doctoral Dissertation, City University London.

Ou, C.Y., Hsieh, P.G., and Chiou, D.C. (1993). "Characteristics of ground surface settlement during excavation." *Canadian Geotechnical Journal*, **30**, 758-767. https://doi.org/10.1139/t93-068

Schanz, T., Vermeer, P., and Bonnier. P. (1999). "The hardening soil model: Formulation and verification." *Beyond 2000 in Computational Geotechnics*, 281-296.

Surarak, C., Likitlersuang, S., Wanatowski, D., Balasubramaniam, A., Oh, E., and Guan, H. (2012). "Stiffness and strength parameters for hardening soil model of soft and stiff Bangkok clays." *Soils and Foundations*, **52**, 682-697. https://doi.org/10.1016/j.sandf.2012.07.009

Zdravkovic, L., Poots, D.M., and St. John, H.D. (2005). "Modelling of a 3D excavation in finite element analysis." *Geotechnique*, **55**(7), 497-513. https://doi.org/10.1680/geot.2005.55.7.497